MONITORING OF SOLAR FAR ULTRAVIOLET RADIATION FROM THE OSO-5 SATELLITE

William A. Rense and Robert Parker
Laboratory for Atmospheric and Space Physics
University of Colorado
Boulder, Colorado 80302

September 1972

Final Report for Period June 1964 - September 1972

Prepared for

GODDARD SPACE FLIGHT CENTER

Greenbelt, Maryland 20771

I

35 pp

TECHNICAL REPORT STANDARD TITLE PAGE

1. Report No.	2. Government Accession No.	3. Recipient's Catalog No.
Final Report		

4. Title and Subtitle	5. Report Date
Monitoring of Solar Far Ultraviolet Radiation from the OSO-5 Satellite	September, 1972
	6. Performing Organization Code
7. Author(s)	8. Performing Organization Report No.
William A. Rense and Robert Parker	
9. Performing Organization Name and Address	10. Work Unit No.
Laboratory for Atmospheric and Space Physics University of Colorado Boulder, Colorado 80302	11. Contract or Grant No. NAS 5-3931
	13. Type of Report and Period Covered Final Report, June, 1964 - Sept. 1972
12. Sponsoring Agency Name and Address	14. Sponsoring Agency Code
Goddard Space Flight Center Greenbelt, Maryland 20771	

15. Supplementary Notes

16. Abstract

A spectrophotometer for monitoring the solar EUV in three broad wavelength bands is described. The kind of data obtained, along with sources of error, are presented. The content of the tape library which contains the data is outlined. The scientific results are discussed. These include: solar flares in the EUV, solar eclipse observations in the EUV, SFD's and relationship to solar flares, and the application of satellite sunrise and sunset data for the study of model upper atmospheres for the earth.

17. Key Words (Selected by Author(s))	18. Distribution Statement
Solar ultraviolet radiation; Solar flares; Solar activity; Composition of earth's upper atmosphere	

19. Security Classif. (of this report)	20. Security Classif. (of this page)	21. No. of Pages	22. Price*
Unclassified	Unclassified	38	

*For sale by the Clearinghouse for Federal Scientific and Technical Information, Springfield, Virginia 22151.

II

Preface

The main objective of the work was to monitor the solar EUV from a wheel instrument on OSO-5. The instrument as finally designed, constructed, and calibrated, was a spectrophotometer utilizing a concave grating and three photomultiplier tubes. The latter detected radiation in three broad wavelength channels, respectively: 1) 280-370 Å, 2) 465-630 Å, and 3) 760-1030 Å. The pulses due to the EUV photons striking the photomultipliers were amplified, shaped and counted. Detection occurred for 30 milliseconds during each revolution of the wheel. The spectrophotometer was turned on for several orbits each day, and obtained usable data from launch (January 21, 1969) through June 1971.

Data were obtained for three large solar flares (March 12, 21 and April 21, 1969). The variation of EUV intensity with time was quite similar for all three bands, and, for the April 21 flare, for which hard X-ray data were available, resembled closely the time variation of the latter. Impulsive peaks were observed for all three bands, superimposed on a rapid rise to maximum and slow decline. Band 3, the one containing photons of highest energy, showed much less tendency for exhibiting these impulsive components. A model of a large flare is proposed based on the OSO-5 EUV data and the concept of twisted magnetic fields around sunspot groups brought on by differential rotation of the sun.

Observations of a partial solar eclipse in the three EUV bands gave some information on the brightness of active areas in EUV, and on the presence or absence of limb-brightening.

Data on the time variation of EUV intensity during sunrise or sunset, for each wavelength band, were compared with the variation predicted from the prevailing CIRA 1965 model atmosphere. For sunset, the predicted curves could be brought into agreement with the observations of all three bands by a modification of the CIRA atmosphere involving a lowering of atomic oxygen density and an increase of molecular nitrogen density.

Contents

Illustrations

I. Objective

The objective of the work of this contract was to a) design, construct and calibrate a spectrophotometer for monitoring the EUV radiation from the sun in three broad bands, b) obtain data with the spectrophotometer from the wheel of the OSO-5 satellite and reduce this data to convenient form, and c) analyze some of the more important data to obtain scientific information about the sun and the earth's upper atmosphere.

II. Introduction

The design of the spectrophotometer for accomplishing the above objectives began in 1964 under contract NAS 5-3931 (June 25, 1964). The choice of the three broad bands to be monitored in the solar EUV was made on the basis of their usefulness as a means of obtaining information on the densities of air at higher levels in the earth's atmosphere and their importance in helping to understand such solar phenomena as flares, enhanced emission from active areas, and long range time variation of solar EUV. Some thought was given to the possibility of designing the spectrophotometer for monitoring only some of the brighter EUV lines in the solar spectrum, but the decision to monitor the bands instead was made on the basis of 1) greater reliability of the instrument and associated electronics because of the higher intensity of the radiation and 2) need at the time for examining solar intensity variation for the entire EUV. Although the three broad bands finally chosen did not cover the entire EUV, they did represent most of the EUV radiant energy below 1030 Å. These bands are: channel 1: 280-370 Å; channel 2: 465-630 Å; and channel 3: 760-1030 Å. Channel 1 contains strong emission lines such as He II (304 Å), Mg IX (368 Å), Fe XVI (335 Å) and Fe XV (284 Å). Channel 2 includes such lines as He I (584 Å); O V (630 Å); Mg X (625 Å and 610 Å); Si XII (500 Å), Ne VII (465 Å) and He I continuum. Channel 3 contains the hydrogen Lyman continuum, the hydrogen Lyman series lines from Lyman beta (1026 Å) to shorter wavelengths, C III (977 Å), O III and O II (834 Å), O IV (790 Å) and Ne VIII (770 Å).

The instrument itself, to assure sufficient speed in the far EUV, was chosen to be a grating spectrophotometer of the grazing-incidence (Rowland circle mount) type. The detection of the EUV was to be made with photomultipliers, one for each wavelength band. The photomultiplier bursts, produced by EUV photons, were to be electronically counted in a suitable way. Radiation from the entire solar disc was to be allowed to enter the spectrophotometer aperture for each revolution of the OSO satellite wheel.

III. Instrumentation

A. Structural Features

The spectrophotometer has the appearance of a truncated, pie-shaped unit made of an aluminum sandwich structure. (Fig. 1). The main spacecraft connector and its cable are mounted on the back wall of the instrument. The back wall and the top are perforated with a pattern of small holes which serve to outgas the instrument in flight. The bottom side of the instrument is made of 1/2 inch aluminum plate containing threaded holes for fastening the instrument to the deck of the spacecraft. The two side walls are made of relatively thin, reinforced aluminum sheet. The front face has a highly reflective surface finish to thermally decouple the instrument from the front panel of the spacecraft. All other exterior surfaces are blackened for efficient radiative coupling to the inner walls of the spacecraft compartment.

The interior of the instrument contains the optical parts and the detection system with associated electronic components.

B. Optics

The optical layout of the spectrophotometer is shown in Figure 2. Light from the entire solar disk enters the slit A and, at a grazing angle of 80°, strikes the concave, 20 cm radius, 1200 line/mm grating G where the EUV in the three wavelength bands are diffracted and brought to focus along the Rowland circle. Three Bendix M 306 resistant strip photomultipliers (1,2,3) receive the three first-order bands, respectively. The EUV which is detected by photomultiplier 2 is first reflected by the mirror M, but the other two beams pass through apertures in the Rowland circle before striking the tube cathodes. Light at the central image is trapped at C. The apertures restrict the geometrical size of each beam, and limit the wavelengths in the bands. The latter limits are: 280-370 Å (Channel 1), 465-630 Å (Channel 2), and 760-1030 Å (Channel 3).

Channel 1 in practice was free of overlapping spectral orders because of of the insensitivity of the spectrophotometer for wavelengths less than about 280 Å. Channels 2 and 3, however, include higher order wavelength radiation

Figure 1.

Photograph of Spectrophotometer

4a

Figure 2.

Optical Layout of Spectrophotometer

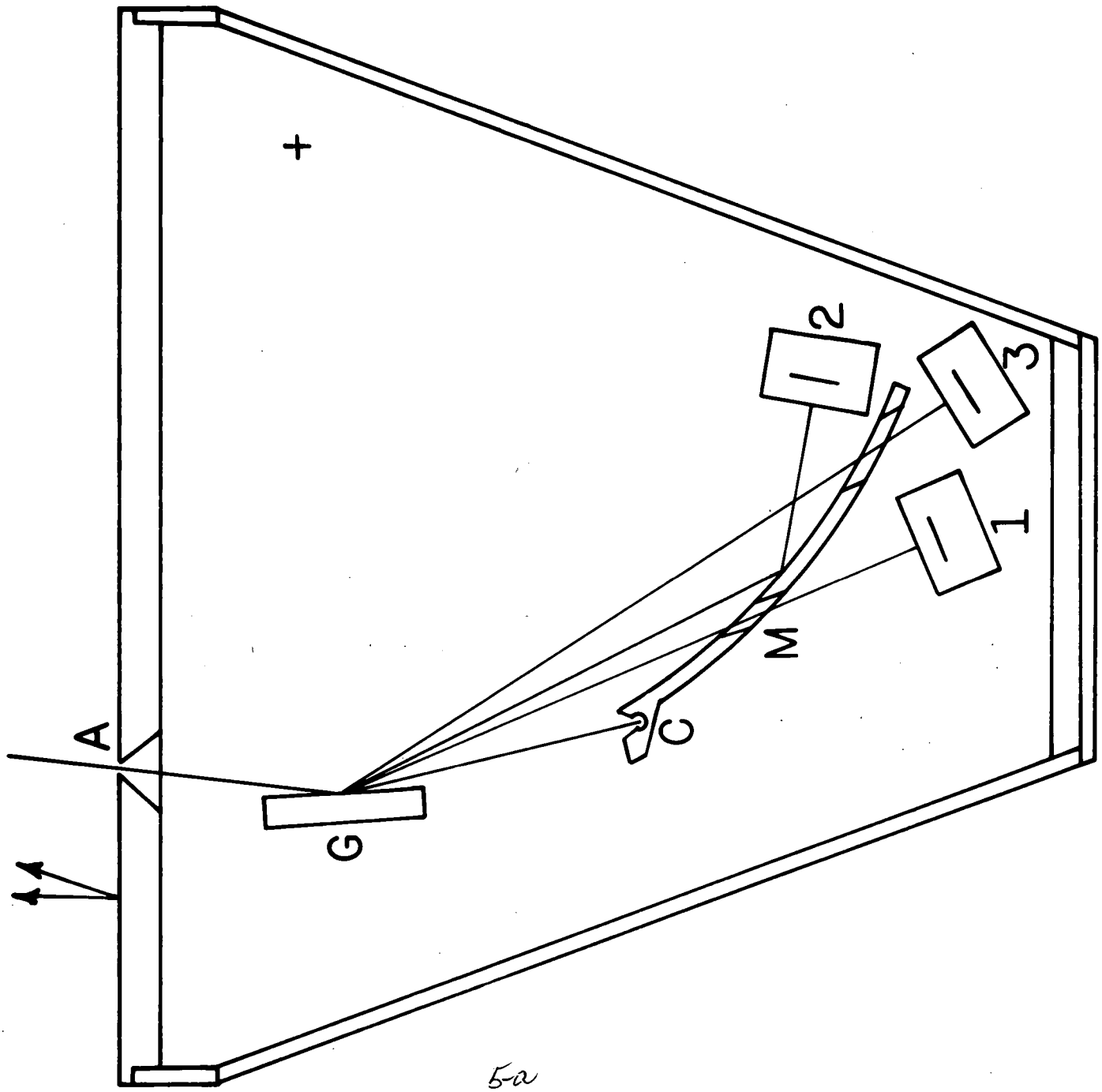

5a

outside their proper ranges; these effects had to be allowed for by the calibration process.

C. Detection

Three Bendix M 306 resistance strip photomultipliers are the basic detectors, one for each EUV wavelength band (or channel). The pulse signals from these photomultipliers are amplified and then shaped. The shaped pulses are sent through electronic gates to a combination of three binary counters and shift registers where they are stored. Counting takes place only when the electronic gate is open. The gate is opened when the sun activates an indexed solar eye unit which is fixed on the outboard wall of the instrument. During this interval (two are possible: 30 millisec or 10 millisec) the sun is illuminating the spectrophotometer grating. After the gate closes, stored counts for each channel are read out to the telemetry and the counters reset to zero. The count range is from 100 to 20,000. The trigger eye optics consists of a cylindrical lens, two glass filters and two photo-resistive diodes. Following read-in, there is a delay ranging from 120 to 310 milliseconds while the commutator is synchronized with the digital telemetry system. One read-out gate is used to acquire synchronization.

For read-out of solar data a sequence of 10 mainframe words is necessary. The first data word is a code word consisting of eight binary "ones." Words 2 and 3 contain the 16 bit binary number stored in the counter for channel 1. The number is read out starting with the least significant bit and proceeding, in sequence, to the most significant bit. Words 4 and 5 contain the intensity data from channel 2; words 6 and 7, from channel 3. Words 8, 9 and 10 contain the eight least significant bits from the background readings of the three channels, respectively. Zeros are now presented to the telemetry system until the next read-in has been completed. When the instrument is calibrated, the read-out sequence is the same as that above, except that the code word now consists of a binary "zero" followed by seven binary "ones." Data read-out is on Main Frame data words 15 and 27.

Five housekeeping channels are used. Analog subcom channels 1, 2, and 3 monitor a voltage proportional to the low voltage supplied to each of the

three detector high voltage supplies in data channels 1, 2, and 3 respectively. Housekeeping channels 4 and 5 monitor temperature probes; the first probe is in the vicinity of the electronics, the second, near the photomultipliers. The analog subcom is read out on Main Frame data word 25.

The command allocation is as follows:

Command No.	Function	Code Format
19	Turns on equipment	0414
11	All high voltage off	0305
113	Channel 2 H.V. on	0309
114	Channel 3 H.V. on	0310
215	Channel 1 H.V. on	0312
202	Calibrate - 4 per hour	0107
229	Calibrate - 1 per hour (30 ms)	0609
132	Calibrate - 1 per hour (10 ms)	0701

D. Calibration

The purpose of the calibration of the spectrophotometer was to provide a means of converting the output of a given channel in terms of counts to an output in terms of absolute intensity of the EUV solar radiation associated with that channel (that is, one of the three wavelength bands).

The vacuum system for calibration (Figure 3) consisted of three separate chambers connected by 6" gate valves: 1) the main chamber which holds the instrument positioned on a rotating table to simulate the rotation of the satellite, 2) the monochromator chamber containing the high voltage capillary discharge source, and 3) the grating chamber. The gases used in the capillary discharge source were hydrogen, helium, argon and xenon in order to provide a range of appropriate wavelengths. A three-stage differential pumping system was required to assure the necessary degree of vacuum in the main chamber. The

Figure 3.

The Calibration System

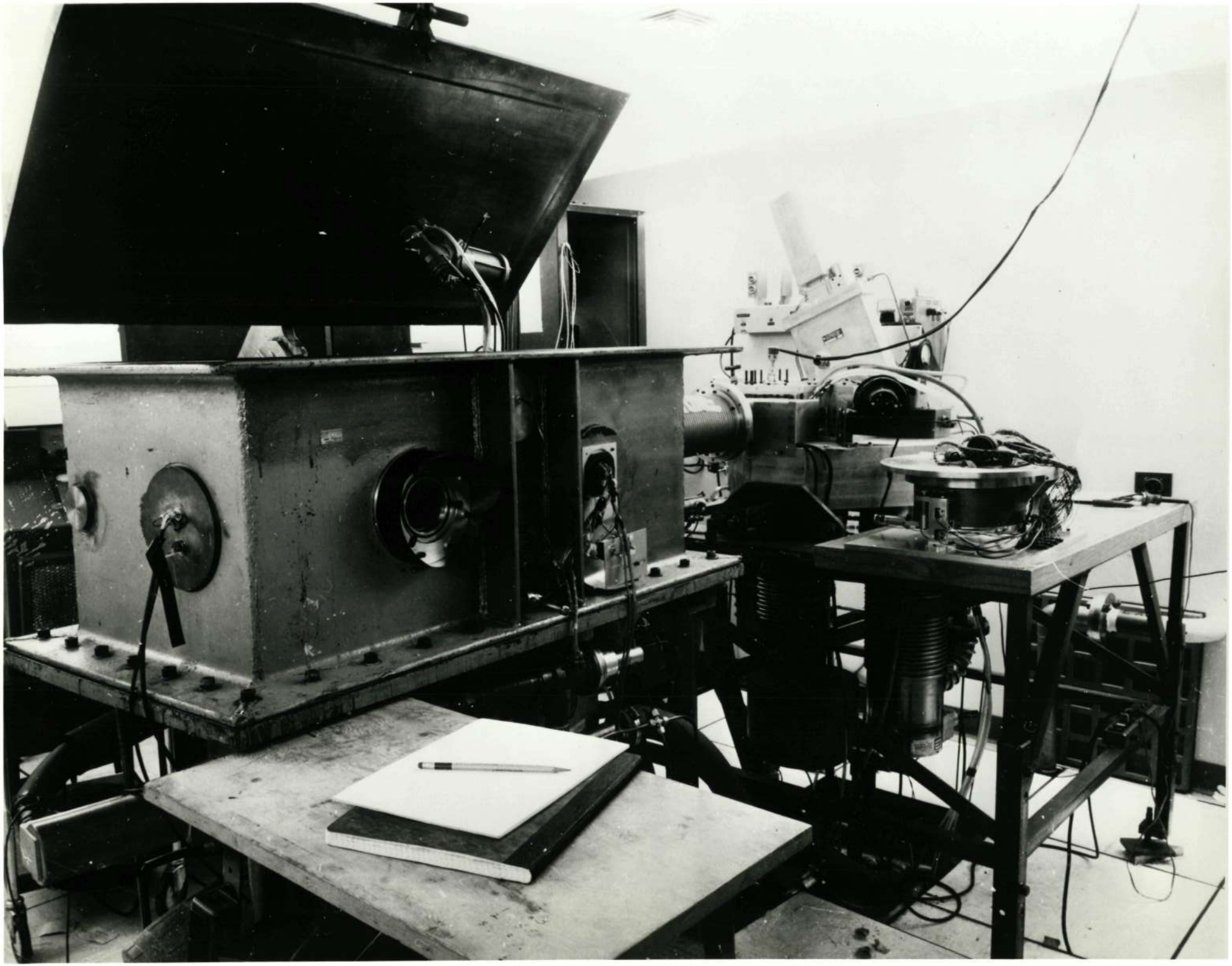

8a

concave grating, serving as the dispersing element, may be rotated so as to select the wavelength falling on the instrument. A series of apertures collimates the light from the source before the light reaches the grating, so that, as viewed from the instrument, the monochromatic beam from the grating corresponds to a source that subtends an angle of 32°. The grating can be replaced by a suitable concave mirror when "white" light is desired. Detection was accomplished by means of a flow-through ion chamber; the current produced by the ionization of the gas in the latter chamber was measured and the absolute intensity of EUV radiation energetic enough to ionize the given gas was computed. A photomultiplier detector at the end of the ion chamber enabled the experimentor to determine when all the EUV radiation passing through the chamber was absorbed in the chamber.

The calibration set-up described above gave sufficient flexibility in wavelength band selection to determine the constants required to convert counts from each wavelength channel of the satellite spectrometer detection system into absolute intensity of the EUV radiation (for that channel) striking the optical aperture of the spectrometer. Nine constants are required as outlined below.

To allow for first order and overlapping order effects, the number of counts S_i' of channel i can be represented by:

$$S_i' = K_{i1} I_1 + K_{i2} I_2 + K_{i3} I_3$$

where I_1, I_2 and I_3 are the actual intensities of the radiation in the three channels, incident on the spectrometer, and K_{i1}, K_{i2}, K_{i3} are constants which are determined by the calibration procedure. The matrix equation:

$$(S') = (K)\ (I)$$

may be inverted to obtain (I):

$$I = (K)^{-1}\ (S')$$

The values of the constants (K's) as determined in the laboratory when used for the actual solar observations from the satellite did not yield realistic values for the intensities of channel 2 and channel 3 but the results for channel 1 were

in good agreement with measurements made by other observers. Accordingly, for convenience in interpreting data, the K's were altered so that reduction to absolute intensities was made to conform to the Hinteregger's values:

$$I_1 = 8.99 \times 10^9 \text{ photons/cm}^2\text{/sec}$$

$$I_2 = 4.40 \times 10^9 \text{ photons/cm}^2\text{/sec}$$

$$I_3 = 20.4 \times 10^9 \text{ photons/cm}^2\text{/sec}$$

The matrix used in such reduction is:

$$\begin{bmatrix} S'_1 \\ S'_2 \\ S'_3 \end{bmatrix} = \begin{bmatrix} 4.31 & 0 & 0 \\ 3.66 & 11.2 & 0 \\ 0.371 & 0.372 & 1.88 \end{bmatrix} \times 10^{-7} \begin{bmatrix} I_1 \\ I_2 \\ I_3 \end{bmatrix}$$

Before applying the above matrix to compute absolute values, the actual observed counts, S, were corrected to obtain S'. The correction involved two steps: first, the elimination of scattered light, and second, the allowance for degradation since launch time. The scattered light, mostly the 1216 Å radiation of the solar hydrogen Lyman alpha line, was measured by observing the sunrise data of each channel. The degradation correction was made by empirically fitting a suitable analytic expression for each channel to the observed curves: average count at spacecraft noon versus time. A source of error which could not be systematically accounted for was pitch of the spacecraft.

In order to have an in-flight check on the performance of the spectrophotometer, a calibration lamp was included in the instrument. The lamp was a sapphire-windowed glass capillary tube containing Xenon gas and operated by a high voltage supply. The ultraviolet radiation emitted falls on the cathodes of the three photomultipliers and produces an output in the form of counts. Changes with time in the sensitivity of the cathodes or in the response of the electronic components associated with the amplification of signal and the subsequent counting system could be monitored in this way. The detection system can be checked by exciting the lamp every 256 or 1024 revolutions of the wheel (determined by command).

IV. Data Reduction

A. Data Sequence

Counts for each channel are obtained for 30 milliseconds when the sun is in the field of view. The counters are then read out to the telemetry and reset to zero. A background count (usually zero) is then made with the sun out of the field of view and the counters again read out to telemetry. The cycle is then completed until initiated by the next pulse from the monitoring eye.

For a few weeks after launch, data from the calibration lamp in the form of counts were obtained every 1024 revolutions of the wheel. Because of a malfunction, these data were discontinued. Later (May 1969) another malfunction in the calibration unit required that the data henceforth be activated by command.

One orbit storage on s/c tape recorders is made for playback to ground stations. For each channel the solar data appear as two 8-bit binary words serially each revolution of the wheel.

In general, to prolong the period of data-taking despite degradation, data are acquired for three consecutive orbits out of every fifteen per day. Useful data have been collected for the period January 23, 1969 to July 19, 1971, spanning about 14,000 orbits of the satellite. This date was chosen because by that time the degradation of the instrument response for EUV wavelength bands 1 and 2 was quite advanced, and that of band 3 moderately advanced. The noise effects were not reduced proportionately, so that measurements during flares, satellite sunrises, and satellite sunsets were not of sufficient quality to justify further reduction of data.

B. Data Library

The tape library of data acquired for the period January 23, 1969 to July 19, 1971 consists of the following:

1. 1068 quicklook tapes
2. 191 correlated data tapes
3. 178 main frame data tapes
4. 46 command history tapes
5. 137 merged data tapes

6. 28 final merged data tapes

7. 289 scratch tapes

8. 1 tape of condensed data from 13,000 orbits

The printed output library consists of:

1. 14 binders containing label information from direct output of the OSO-5 program (1,000 orbits or CDT files per binder)
2. 2 binders containing selected information on each orbit
3. 2 binders of label information, via the merged program, for each re-formatted file on the merged data tapes
4. 1 binder containing the above three items of information for data of poorer quality which was not placed on the final merged data tapes
5. 1 binder containing printout of the punched output from the OSO-5 program
6. 1 binder containing output of the catalog program which shows orbit number vs. file number for the correlated data tapes
7. 1 binder containing computer program listings for all the auxillary programs as well as main programs for OSO-5

In addition there are 13 boxes of punched output from the OSO-5 program containing condensed data for about 1,000 orbits, and 6 boxes of OSO-5 main and auxillary program decks. A 500 page volume includes the documentation of all OSO-5 computer programs which were written for the handling and analysis of all the data.

C. Data Presentation and Error Analysis

A graph of observed noon-day counts vs. orbit number for all three channels is shown in the lower graph of Figure 4. From top to bottom, the sets of points refer, respectively, to channels 3, 1, 2. Many of the irregularities in these curves are not real. The gradual degradation of each channel is quite apparent, as are the breaks where no data were obtained (instrument off). All of the data counts were acquired in a 30 millisec interval. Other variations in the curves may be attributed to 1) pitch of the satellite, 2) interaction of raster

Figure 4.

Sample Data, EUV vs. Time

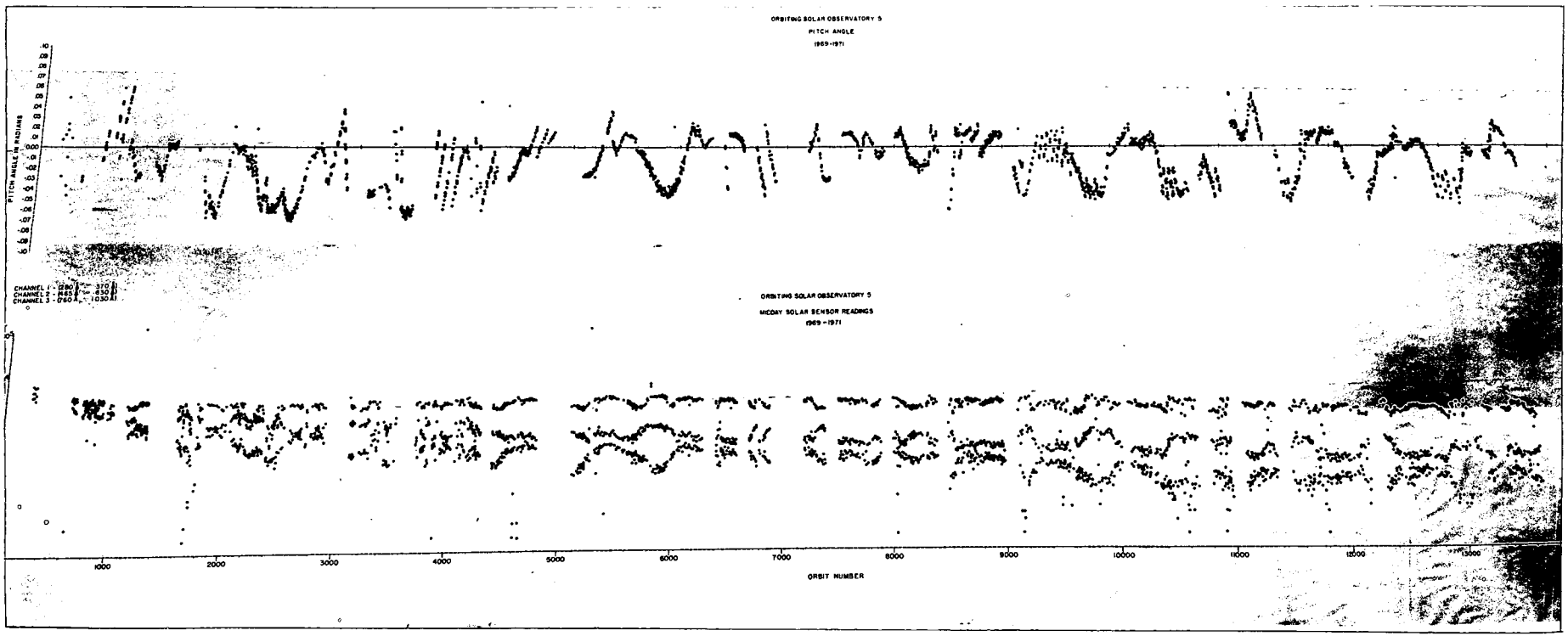
ORBITING SOLAR OBSERVATORY 5
PITCH ANGLE
1969-1971
PITCH ANGLE IN RADIANS
ORBITING SOLAR OBSERVATORY 5
MCDAY SOLAR SENSOR READINGS
1969-1971
1000
2000
3000
4000
5000
6000
7000
8000
9000
10000
11000
12000
13000
ORBIT NUMBER

13a

scanning of the pointed instruments on the satellite, 3) intrinsic variation in instrument response, 4) actual variations in the solar EUV intensity for each channel. Each of these will be considered.

A graph of the monitored values of satellite pitch at noon vs. orbit number is shown in the upper graph of Figure 4. This curve does not show short period pitch changes which sometimes also occurred. An effort to find a systematic quantitative relationship between the curves in Figure 4 was unsuccessful. In general, channel 1 intensity increases for large negative pitch, and that for channel 2 decreases. A change in pitch would cause the solar light to sweep through the instrument aperture at a slightly different angle. Because of the presence of baffles in the optical paths of the three channels, pitch changes could cause variations in the amount of EUV striking the photo tubes. Moreover, if the reflectivity of the grating changed over the area of the grating, and if the photocathode surfaces of the photomultipliers were not uniformly sensitive, pitch effects would be present. For analysis of data for a particular orbit, or fraction of an orbit, pitch changes were normally negligible, and do not alter the observed values of, at least, relative intensity vs. time.

When raster scanning of the pointed instruments on the satellite occurs, the EUV counts from the photomultipliers oscillate in a somewhat regular manner. The effect is only occasionally present and can easily be recognized. It may be nearly completely eliminated by a suitable averaging of intensities over several adjacent points. However, time resolution of the measurements may be reduced when such averaging is required.

An apparently random variation of intensity from point to point is present in each channel. It is least for channel 3. No explanation for this irregularity in response could be found, but it appears to be instrumental. When adjacent intensity points over several consecutive revolutions of the wheel are averaged, a regular variation is observed of period approximately 5 minutes. It is believed that this effect is either instrumental or associated with the satellite environment. A gradual decline in average intensity of the EUV is observed in all cases during the daytime interval after satellite sunrise and before satellite sunset. Again, this effect is believed to be instrumental and is probably the result of

temperature changes. It may also reflect a temporary loss in sensitivity of the photomultipliers over the time of continuous diurnal exposure.

Changes in intensity other than those mentioned above are assumed to be real variations in solar EUV radiation. An example is that of a solar flare. For such variations, after a suitable averaging procedure, relative intensities are normally estimated to be accurate to 2% with a time resolution of about 4 seconds.

V. Science

A. Scope of Science Analysis

Four scientific projects were undertaken and completed in the analysis of the reduced solar EUV data. These are 1) study of large flares, 2) interpretation of solar eclipse EUV data of March 7, 1970, 3) study of relationship between solar EUV flare intensities and sudden frequency disturbances (SFD's), 4) analysis of sunrise and sunset absorption data for comparison with predicted absorption of CIRA model atmospheres for the earth.

The detailed results of the above projects are contained in the papers:

1. "Solar Flares in the EUV Observed from OSO-5," by P. T. Kelly and W. A. Rense, to be published in Solar Physics, September or October, 1972 issue.
2. "Observations of March 7, 1970 Solar Eclipse from OSO-5 in Far UV," by R. Parker and W. A. Rense, Report UAG-2, Part III, (World Data Center A, Upper Atmosphere Geophysics), April, 1971, p. 417.
3. "SFD's for Three Large Solar Flares," by F. Solheim. Thesis in progress for Ph.D. degree, University of Colorado, 1972.
4. "Broad Band Solar EUV Absorption in Upper Atmosphere," by K. Allen and W. A. Rense (to be submitted for publication).

Only a brief summary of some of the results of the above papers will be given here.

B. Solar Flares in the EUV

Solar flares in the three EUV channels were observed for flares of brightness 1B, 2B and 3B. Figures 5, 6 and 7 show the variation of EUV intensity with time for each of the channels for the large flares of March 12, March 21, and April 21, 1969. In general, the time dependence of flare intensity in each band is characterized by a more or less slowly varying component with one or more impulsive bursts superimposed. Channel 2 (465-630 Å) and channel 3 (760-1030 Å) are quite similar in their time variations, but channel 1 (280-370 Å) shows less or no impulsive structure, and declines more slowly. The total time-integrated absolute flare energies for the three channels, 1, 2, and 3, are, respectively, (in units of ergs): March 12, 1.0×10^{29}, 1.4×10^{29}, and $1.3 \times$

Figure 5.

Solar Flare of March 12, 1969

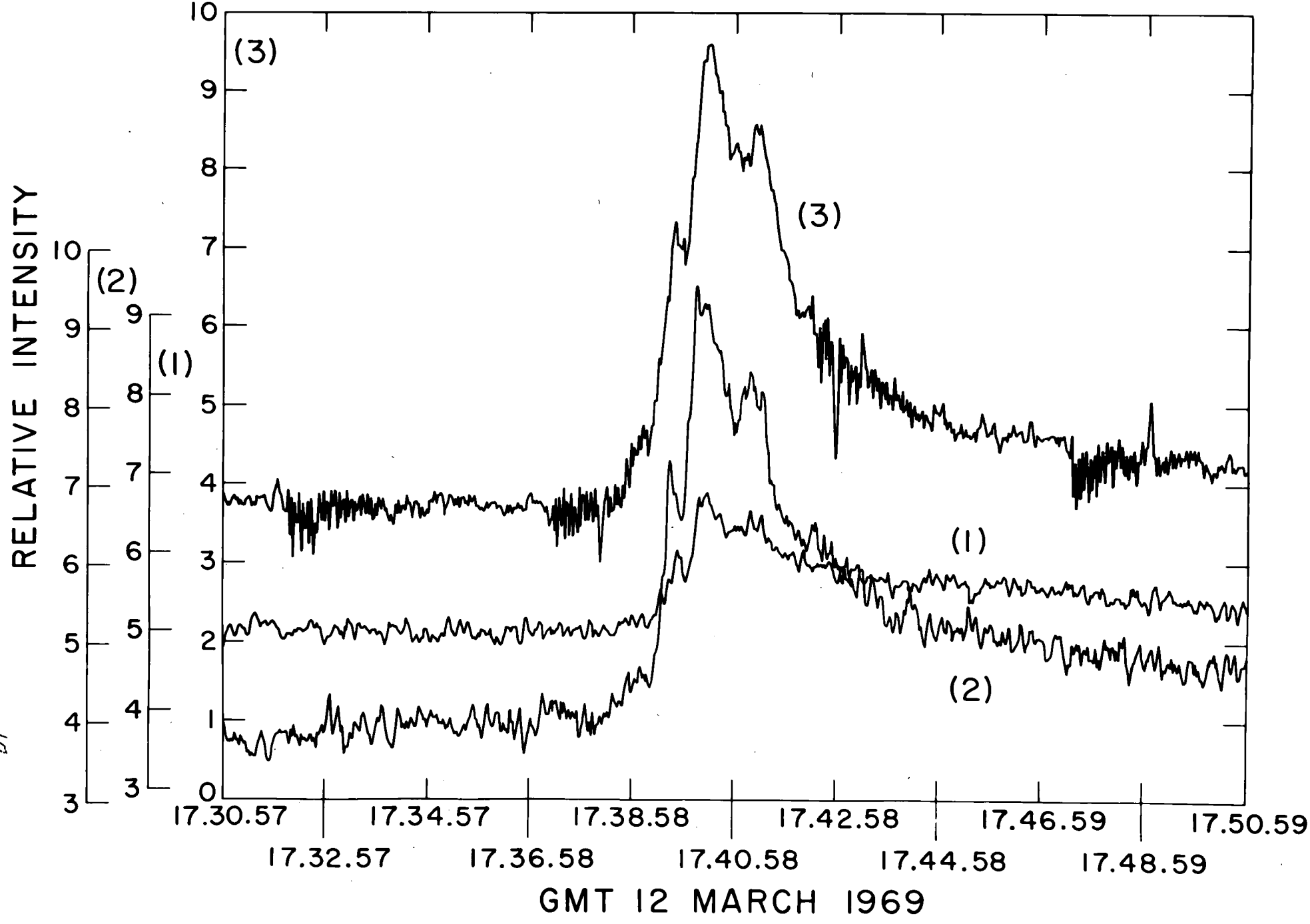
RELATIVE INTENSITY
(3)
(2)
(1)
10
9
8
7
6
5
4
3
2
1
0
17.30.57
17.32.57
17.34.57
17.36.58
17.38.58
17.40.58
17.42.58
17.44.58
17.46.59
17.48.59
17.50.59
GMT 12 MARCH 1969

Figure 6.

Solar Flare of March 21, 1969

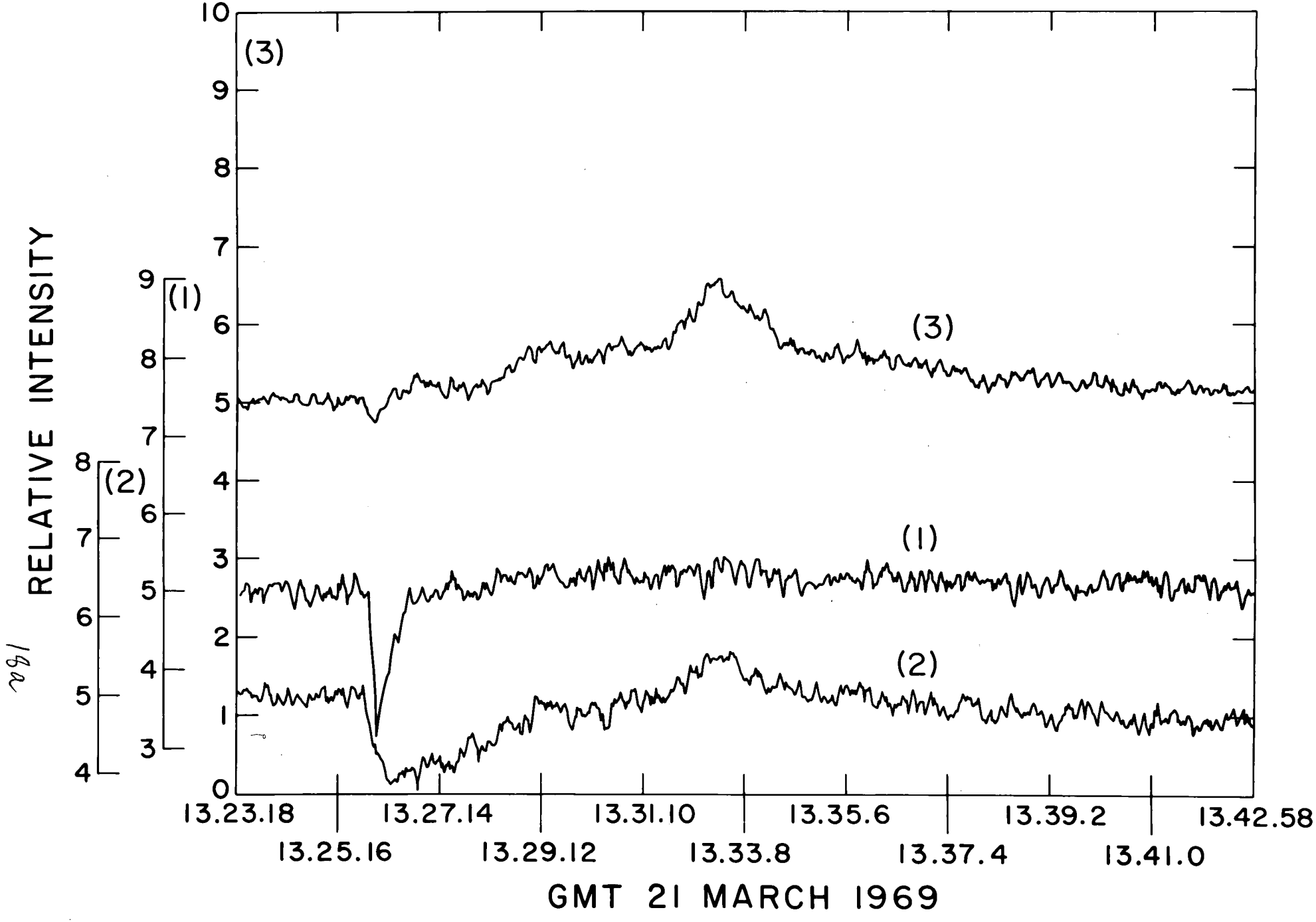
RELATIVE INTENSITY
(1)
(2)
(3)
13.23.18
13.25.16
13.27.14
13.29.12
13.31.10
13.33.8
13.35.6
13.37.4
13.39.2
13.41.0
13.42.58
GMT 21 MARCH 1969

Figure 7.

Solar Flare of April 21, 1969

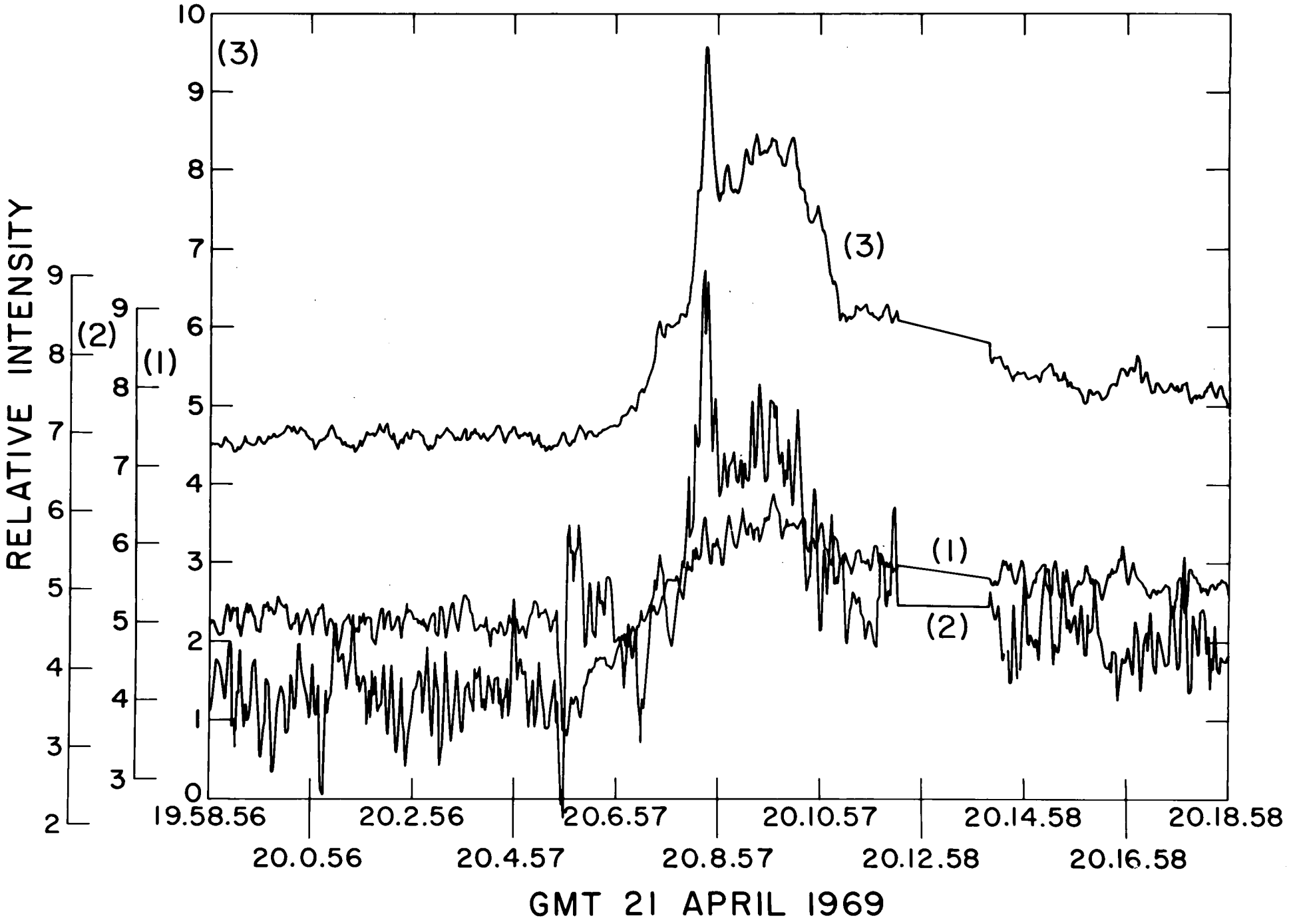
RELATIVE INTENSITY
(1)
(2)
(3)
19.58.56
20.0.56
20.2.56
20.4.57
20.6.57
20.8.57
20.10.57
20.12.58
20.14.58
20.16.58
20.18.58
GMT 21 APRIL 1969

10^{29}; March 21, 7.0×10^{28}, 4.0×10^{28} and $1.3. \times 10^{29}$; April 21, 1.3×10^{29}, 1.6×10^{29} and 2.2×10^{29},

A comparison of available data on 2800/mc/sec radio emission during the above flares led to the conclusion that the onset of the first rapid intensity increase in the radio emission was associated with the first impulsive component of the flare EUV radiation. For the April 21 flare, data on hard X-ray emission was available. The time variation of this X-ray component of the flare was similar in considerable detail to that of the EUV components.

An idealized model of a flare is proposed which accounts for the general characteristics of the time variation in the flare EUV. The model is primarily based on the theoretical investigations of Bessey and Kuperus (5) (Bessey, R. J. and Kuperus, M.: 1969, Conference on Chromosphere - Corona Transition Region, Boulder, Colorado) and of Barnes and Sturrock (6) (Barnes, C. W. and Sturrock, P. A.: 1972, AP. J. 174, p. 659). The first of these papers deals with the dynamic and thermal changes that occur in a mass of solar chromospheric plasma when energy is applied to a thin layer. Their computations show that within 200 seconds, for an energy input of about 10^{12} ergs/gm/sec: 1) the original exponential density distribution is replaced by one that is approximately uniform; 2) upward expansion velocities of as much as 50 km/sec could be produced; 3) shock waves could be formed with material streaming up after the shock. These results apply to an idealized situation with no magnetic field present. However, they apply qualitatively if a magnetic field is present, especially where the latter is nearly perpendicular to the photospheric surface. Barnes and Sturrock (loc. cit., above) consider the case with a magnetic field extending from a sunspot to regions symmetrically surrounding the spot, and of opposite polarity. They calculated the energy in possible force-free fields (resulting from twisting due to differential rotation) which have the same boundary conditions and found that, for a sufficient amount of twisting, the energy in the force-free field can be greater than that in an open field having the same photospheric boundary conditions. They propose that in a flare a force-free field, by a series of explosive processes, may change to an open field of lower energy.

The model described here utilizes the results of the above investigators to explain qualitatively the general features of the EUV radiation emitted during

a large flare. Consider the magnetic field associated with an active spot group after it has been twisted by rotation of the spot center. Then, as mentioned above, its energy is greater than that of the original, untwisted field. This energy comes from that associated with the differential rotation of the sun. Next, suppose that the degree of twisting has proceeded to the point that the closed force-free field has energy greater than that of an open field with the same photospheric boundary conditions, namely, it is in a metastable state as pointed out by Barnes and Sturrock in the paper cited above. If heating in some part of the lower region of the plasma engulfed by the magnetic field produces a local energy input over a critical value, given as 10^{12} erg/g/sec by Bessey and Kuperus, then a shock wave will be produced as found by the latter authors (loc. cit.). The material streaming upward after the shock wave opens the magnetic lines of force and provides the mechanism for the explosive transition from the metastable closed field to the lower energy open field. Magnetic energy is released to the plasma to raise its temperature and to accelerate charged particles. This is the part of the flare which corresponds to the impulsive peaks of the EUV time-variation curves (Figures 5,6, and 7). According to Barnes and Sturrock the energy released could be of the order of one-fifth of that in the original current-free magnetic field. The energy given to a charged particle during this phase averages about 100 keV and may be as high as 10^3 keV. The lines of the open field are then reconnected to form a closed field corresponding to the original undistorted field. The energy here released may be of the order of that in the original field and accounts for the main part of the flare energy (Barnes and Sturrock, loc. cit., and Sturrock (7), Solar Physics, in press, and, for the relativistic particles, C. deJager (8), Utrechtse Sterrekundige Overdrukken, No. 92, 1, 1969).

The triggering of the transition from the closed field metastable state to the open field configuration may be the falling of material in prominences (Ch. L. Hyder (9), Solar Physics, Vol. 2, 1967). Much of the EUV flare radiation could be a result of collisional excitation at lower levels after the release of trapped particles when the magnetic field opens. The hard X-rays originate in the same way, as well as some of the radio emission. Those emissions would be associated with the impulsive part of the flare.

C. Solar Eclipse Observations

The solar eclipse observations of March 7, 1970 led to the following conclusions: 1) limb brightening is present for the integrated EUV radiation in channels 1 and 2 (the higher photon energy channels) but not in channel 3. 2) The active regions in the southern hemisphere were brighter than the surrounding regions by factors 3, 4, and 2 for channels 1, 2, and 3, respectively. In the northern hemisphere the active regions were brighter by factors of 2, 4, and 2, respectively.

D. Sunrise and Sunset Data

EUV absorption in the three channels has been observed during sunrise and sunset as viewed from the satellite. The observations were made in a zone between latitudes $\pm 33^{\circ}$. Typical curves, intensity vs. h, are shown in Figure 8, where h is the perpendicular distance between the satellite-sun line and the earth's surface. This type of variation of integrated intensity for each channel can be predicted from a model atmosphere since the wavelength components of the solar EUV in the channels are known, as well as their absorption coefficients for each important atmospheric constituent. Predicted intensity variations for the prevailing CIRA (1965) atmospheric model of the time of the EUV observations were compared with the latter. Within experimental error, the CIRA models accounted for the observed results for channel 2 over several sunrise and sunset data sets at widely-spaced time intervals. Channel 1 showed slightly greater intensity than predicted by the prevailing CIRA model. Channel 3 data, on the average, showed considerably less intensity than that predicted by the prevailing CIRA model.

In order to account for the observed inconsistency of the channel 3 and channel 1 data with the predictions of the CIRA model, it is necessary for one to assume less atomic oxygen and more molecular nitrogen than given by the prevailing CIRA model. If the CIRA model atmosphere is modified so that the atomic oxygen density is reduced by about one-third, and the molecular nitrogen density increased by about a factor of 2, the modified CIRA model will predict intensities in agreement with all three wavelength channels. The change

Figure 8.

EUV Intensity Variations at Sunset

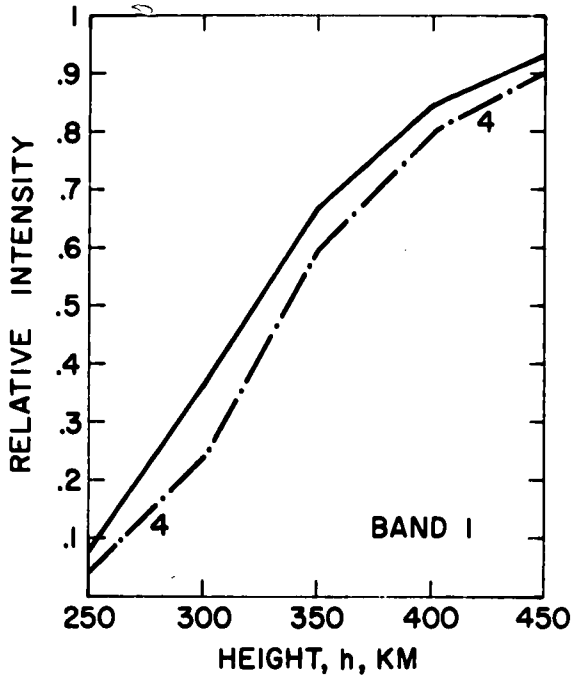
RELATIVE INTENSITY
1
.9
.8
.7
.6
.5
.4
.3
.2
.1
4
4
BAND 1
250
300
350
400
450
HEIGHT, h, KM

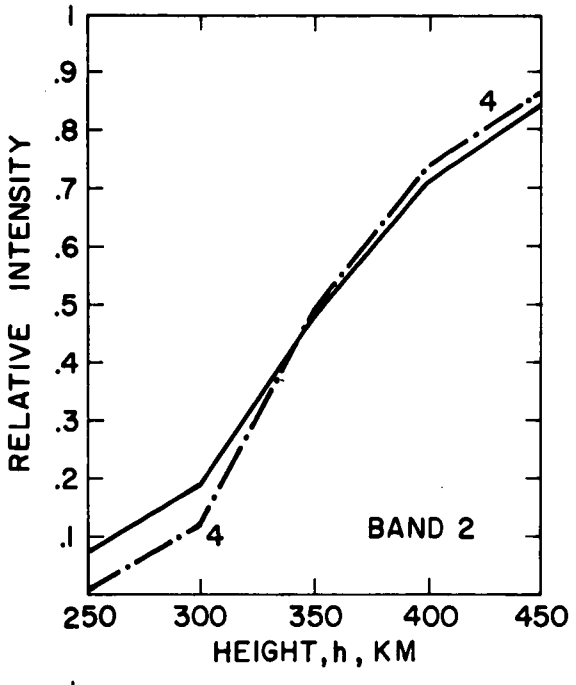
RELATIVE INTENSITY
1
.9
.8
.7
.6
.5
.4
.3
.2
.1
4
4
BAND 2
250
300
350
400
450
HEIGHT, h, KM

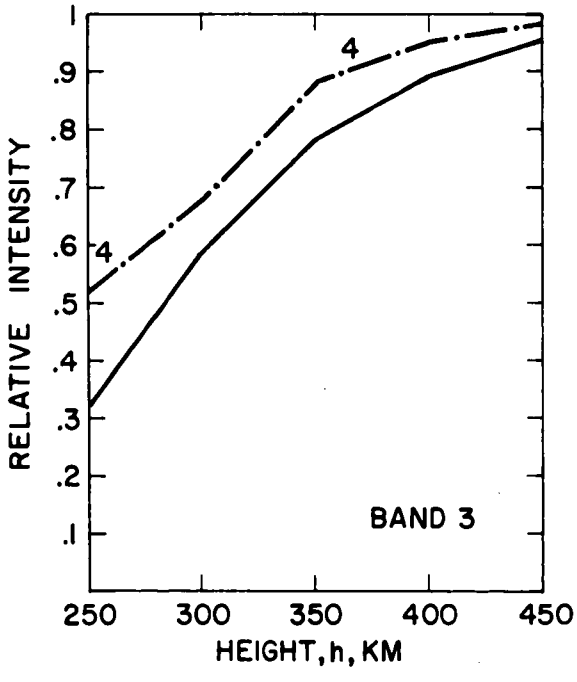
RELATIVE INTENSITY
1
.9
.8
.7
.6
.5
.4
.3
.2
.1
4
4
BAND 3
250
300
350
400
450
HEIGHT, h, KM

has little effect on the overall EUV absorption of channel 2 (where the absorption effects of O and N_2 are comparable) but a large effect (in the correct direction) for channel 3 where absorption by nitrogen dominates. In addition, predicted intensities for channel 1 are slightly greater because this channel is most sensitive to the lowered oxygen density. Other investigators have also observed less atomic oxygen than predicted by the CIRA (1965) model ("Ionospheric Estimates of Atomic Oxygen Concentration from Charged Particle Measurements," Mahajan, K. K., (10), J. Geophys. Res. 76, 4621, 1971).

References

1. Kelly, P. T. and W. A. Rense, "Solar Flares in the EUV Observed from OSO-5," Solar Physics, 1972, to be published.

2. Parker, R. and W. A. Rense, "Observations of March 7, 1970 Solar Eclipse from OSO-5 in Far UV," Report UAG-2, Part III, World Data Center A, Upper Atmosphere Geophysics, April, 1971, p. 417.

3. Solheim, F., "SFD's for Three Large Solar Flares," Thesis, University of Colorado.

4. Allen, K. and W. A. Rense, "Broad Band Solar EUV Absorption in Earth's Upper Atmosphere," submitted for publication in J. Geophys. Res., 1972.

5. Bessey, R. J. and M. Kuperus, 1969, Conference on Chromosphere-Corona Transition Region, Boulder, Colorado.

6. Barnes, C. W. and P. A. Sturrock, "Force-Free Magnetic-Field Structures and Their Role in Solar Activity," Ap. J. 174, 659, 1972.

7. Sturrock, P. A., Solar Physics, in press, 1972.

8. DeJager, C., "Solar Flares; Properties and Problems," Solar Flares and Space Research, North-Holland, Amsterdam, 1969.

9. Hyder, C. L., "A Phenomenological Model for Disparitions Brusques Followed by Flarelike Chromospheric Brightenings," Solar Physics 2, 267, 1967.

10. Mahajan, K. K., "Ionospheric Estimates of Atomic Oxygen Concentration from Charged Particle Measurements," J. Geophys. Res. 76, 4621, 1971.

Acknowledgements

The research described in this report is the result of the work of many people. The authors acknowledge, in particular, the early contributions made by Edward P. Todd and Claire E. Sheldon. Elmo C. Bruner, Jr., contributed significantly to the calibration program and the formulation of scientific objectives. Stephen A. Bundy carried out most of the laboratory optical and calibration work. The basic design and construction of the instrument was accomplished by personnel in the LASP engineering design and shop groups under the direction of Kermit A. Gause and Berthold Glatt. Hassan Bahrami along with Michael Oppenheimer and Kevin G. Jones were responsible for much of the electronics design, assembly, and testing. Richard C. Branan, Mary Lou Dick, M. Murbach and Maureen J. Anderson participated in the initial phases of the data reduction program. The authors are especially grateful to Ronald O. Williams for the bulk of the work involved in the programming and tape-merging procedures required for data reduction and the assembly of the tape library.